

Fermionic correlations as metric distances: A useful tool for materials science

Simone Marocchi,¹ Stefano Pittalis,² and Irene D’Amico^{1,3}

¹*Instituto de Física de São Carlos, Universidade de São Paulo, CP 369, 13560-970, São Carlos, SP, Brazil.**

²*CNR-Istituto di Nanoscienze, Via Campi 213A, I-41125 Modena, Italy[†]*

³*Department of Physics and York Centre for Quantum Technologies,
University of York, York YO10 5DD, United Kingdom[‡]*

(Dated: July 28, 2021)

We introduce a rigorous, physically appealing, and practical way to measure distances between exchange-only correlations of interacting many-electron systems, which works regardless of their size and inhomogeneity. We show that this distance captures fundamental physical features such as the periodicity of atomic elements, and that it can be used to effectively and efficiently analyze the performance of density functional approximations. We suggest that this metric can find useful applications in high-throughput materials design.

PACS numbers: 31.15.E-, 31.15.V-, 71.15.Mb, 03.65.-w

I. INTRODUCTION

The discovery of innovative materials and engineering devices with targeted properties involve substantial experimental and theoretical efforts. Their progress ultimately relies on our understanding of the physics at the nanoscale. Atomistically, the possible constituents and their combinations are vast. One can often focus on the state of electrons within the Born-Oppenheimer approximation, however a too direct computational approach is in general unpractical, because of the presence of many degrees of freedom and the fact that these are interrelated in a non-trivial fashion. Density functional theory (DFT) proposes an alternative by transforming the problem of determining interacting many-body system properties into the solution of the Kohn-Sham (KS) equations, which only involve auxiliary non-interacting particles [1–3]. Practically, the KS approach relies on the possibility of devising approximate forms for the exchange-correlation (xc) energy – a functional of the particle density. This functional embodies the effects of many-body correlations due to the intrinsic anti-symmetry of the many-electron state and to the electrostatic electron-electron repulsions; it also accounts for the auxiliary KS system being non-interacting. Within this context, we wish to expose the usefulness of introducing metric spaces to analyze many-body correlations – when the protocol to define these spaces is both rigorous and based on quantities with a deep physical meaning.

There is an increasing interest in the use of metrics to explore quantum mechanical systems [4–10], and appropriate (“natural”) metrics for particle densities, wavefunctions, and external potentials [4, 7] already shed light on (previously unknown) features of the mappings at the base of the Hohenberg-Kohn theorem, the cornerstone of DFT. Among the ultimate goals of DFT applications is the determination of properties such as total energies, ionization potentials, electron affinities, the fundamental

gaps, and lattice distances of crystalline structures. All these quantities can be computed accurately only if the relevant two-body correlations are properly captured by the underlying approximations. The xc energy, at the core of the KS DFT approach, can be expressed in terms of the aforementioned two-body correlations by means of the xc-hole function as defined in the so-called adiabatic coupling-constant integration [1–3]. Furthermore, the xc hole can be split into a correlation (c) and an exchange (x) component. Here, we focus on an exchange-only analysis of this quantity (more details follow below), which is useful for dealing with relatively weakly correlated systems’ ground states. First, we will introduce a “natural” distance for the x hole and show that it captures fundamental physical features such as the periodicity of atomic elements; afterwards we will also demonstrate that it can be used to effectively and efficiently analyze the performance of density functional approximations.

II. METRIC SPACE DESCRIPTION OF EXCHANGE HOLES

Let us briefly remind the reader of a few fundamental definitions [11]. The exchange-hole (x hole) has an expression

$$n_x(\mathbf{r}, \mathbf{r}') = -\frac{\sum_{\sigma} |\gamma_{\sigma}(\mathbf{r}, \mathbf{r}')|^2}{n(\mathbf{r})} \quad (1)$$

which can be evaluated once the KS one-body reduced density matrix (1BRDM)

$$\gamma_{\sigma}(\mathbf{r}, \mathbf{r}') = \sum_k f_{k\sigma} \psi_{k\sigma}(\mathbf{r}) \psi_{k\sigma}^*(\mathbf{r}') \quad (2)$$

is known. This, in turn, only requires the knowledge of the *occupied* single-particle orbitals $\psi_{k,\sigma}(\mathbf{r})$. Here, $f_{k\sigma}$ are occupation numbers and σ is the z projection of the spin index [12]. At the denominator of

Eq. (1), the particle density is determined from the trace $n(\mathbf{r}) = \sum_{\sigma} \gamma_{\sigma}(\mathbf{r}, \mathbf{r})$. Note that the calculation of the x energy, E_x , can be based on the knowledge of the system-averaged x hole, $\langle n_x \rangle$, as follows:

$$E_x = 2\pi \int_0^{\infty} u du \langle n_x \rangle(u) \quad (3)$$

where

$$\langle n_x \rangle(u) := \int d\mathbf{r} n(\mathbf{r}) n_x(\mathbf{r}, u), \quad (4)$$

with

$$n_x(\mathbf{r}, u) := \frac{1}{4\pi} \int d\Omega_{\mathbf{u}} n_x(\mathbf{r}, \mathbf{r} + \mathbf{u}) \quad (5)$$

being the spherical average of the x hole, and $\Omega_{\mathbf{u}}$ being the solid angle defined by \mathbf{u} around \mathbf{r} . Therefore, practical calculations in DFT can be enabled by providing approximations for $\langle n_x \rangle(u)$. Sensible approximations must satisfy important exact conditions. In this respect, it is well known that the property

$$\int_0^{\infty} 4\pi u^2 du \langle n_x \rangle(u) = -N \quad (6)$$

together with the pointwise negativity condition are of utmost importance. These two properties can be combined, giving raise to the constraint

$$\int_0^{\infty} 4\pi u^2 du |\langle n_x \rangle(u)| = N. \quad (7)$$

Crucially, through Eq. (7) and by following the protocol for deriving natural metrics of Ref. 5, *these same conditions allow us to define the natural distance* between two given system-averaged x-hole functions,

$$D_x[\langle n_x^{(1)} \rangle, \langle n_x^{(2)} \rangle] := 4\pi \int_0^{\infty} u^2 du |\langle n_x^{(1)} \rangle(u) - \langle n_x^{(2)} \rangle(u)|. \quad (8)$$

Equation (8) is the key result of the present work. We emphasize that the same exact conditions that are essential to explain surprisingly good performance of even very rough DFT approximations, allow us to introduce a rigorous metric: we expect then this metric to capture the essential physics of exchange-only correlations.

Equation (8) summarizes the difference between the exchange-only correlations of two many-body systems into a *single number*. While differences of exchange energies could be thought too as “single numbers” to estimate the difference between the exchange in two systems, Eq. (8) not only rigorously satisfies the mathematical properties of a distance [13] but also enables a comparative analysis of the systems that is far more detailed than the claim that they have the same exchange energy – the examples illustrated below will provide a vivid illustration of this point. By the metrics’ axioms, $D_x = 0$ if and

only if the two systems considered have the *same* system-averaged x hole (modulo irrelevant differences over sets of vanishing measure). For non vanishing distances, Eq. (8) implies a *well-defined maximum*, given by the sum of the two systems’ particle numbers. This can be evinced from Eqs. (8) and (7) by considering two systems of particle numbers N_1 and N_2 for which the system-averaged x holes do not overlap: in this case $D_x = N_1 + N_2$. Because the system-averaged x holes have a definite sign, this also corresponds to the maximum distance between the two systems. This property implies that the x-hole distance between two systems gives us a *non-arbitrary* “absolute” measure of their closeness, as their distance can be recast in terms of a *percentage of their maximum possible distance*.

Furthermore, Eq. (8) implies a very effective geometrical structure of the physical Fock space. Consider the application of Eq. (8) to compute the distance between the *exact* system-averaged x holes of two different systems. This distance represents a measure of the difference of the exchange-only correlations between two systems. A system with no particles may be thought of as a point, say, at the center of the Fock space. Because of Eq. (7), all the other systems will be distributed at a fixed distance equal to the number of particles in the systems. Thus, the overall Fock space can be thought of as the union of disjoint “onionlike” shells: systems with same number of particles are on the same shell; systems whose external potentials differ only by a constant are separated by a vanishing distance (i.e., they occupy the same point) as the orbitals and therefore the 1BDM and corresponding particle densities do not change. Exchange holes and therefore their distances are unchanged if each single-particle orbital is multiplied by the same constant phase. This embodies the fact that both the Schrödinger equation and the DFT framework are invariant under global gauge transformations [14]. Systems will be on different shells if they have different particle numbers: the distances acquire minimum value (i.e., the absolute value of the difference of the shell radii) if the systems “face each other,” and they acquire maximum value (i.e., the sum of the shell radii) if the systems are “on opposite poles” [15]. Of course, the configurations which generate maximum and – for systems on different shells – minimum distances are not unique.

Finally, let us consider the evaluation of Eq. (8) using some approximate $\langle n_x \rangle$. Since Eq. (7) must be fulfilled, proper approximations preserve the mentioned onionlike structure of the Fock space. Also the minimum and maximum distances are unchanged, but the configurations at which these occur may vary from the exact case. The errors due to the approximation may be viewed as fictitious displacements of the systems from their exact locations on the aforementioned shells. Having the possibility to quantify these errors through a rigorously defined distance that can also be visualized is, *per se*, very ap-

peeling. In the rest of this paper, we will give explicit examples of how powerful this approach can be.

III. NUMERICAL RESULTS

We start by considering a set of systems for which the exact x holes can be calculated: we will discuss the exact results as well as compare and contrast these with corresponding results from DFT approximations. Here we shall consider popular approximations for $\langle n_x \rangle$: the local-density approximation (LDA), the generalized gradient approximation (GGA), and the meta-GGA (MGGA). The LDA takes as a reference the xc energy densities of the homogeneous electron gas; GGA and MGGA are nonempirical refinements which aim at capturing the effects of system inhomogeneities – those neglected within the LDA – while progressively satisfying a larger set of exact conditions. LDA forms make use only of the particle density $n(\mathbf{r})$ as input; GGAs also use the reduced dimensionless gradient, $s(\mathbf{r}) = |\nabla n(\mathbf{r})| / \{2 [3\pi^2]^{1/3} n(\mathbf{r})^{4/3}\}$; $n(\mathbf{r})$ and $s(\mathbf{r})$, the kinetic-energy density $\tau = \sum_{k\sigma} f_{k\sigma} |\nabla \psi_{k\sigma}(\mathbf{r})|^2$, and, possibly, the Laplacian of the particle density may be exploited in MGGAs. MGGA forms are then considered to be the most accurate approximations among these three. As representative approximations for $\langle n_x \rangle$, we choose the versions of the Perdew-Wang LDA and of the Perdew-Burke-Ernzerhof GGA by Ernzerhof and Perdew [16] and the version of the Tao-Perdew-Staroverov-Scuseria MGGA by Constantin et. al [17].

Figure 1 shows the distances of the exact $\langle n_x \rangle$ (solid line) from a reference system chosen (arbitrarily) at $Z^{ref} = 50$ for the isoelectronic heliumlike sequence [18]. Distances from the reference system increase monotonically for both increasing and decreasing values of Z . As the distance increases, the spatial overlap of the related system-averaged x holes decreases. The system-averaged x holes $\langle n_x(u) \rangle$ describe the system-averaged electron depletion observed at separation u from a reference electron due to the effect of electron-electron exchange, so an increasing distance D_x implies systems with an increasingly different spatial exchange pattern. When there is no overlap between these patterns, their distance saturates at its maximum, which is $D_x^{max} = 4$ for the set of systems of Fig. 1. Next we check how the trend for the exact exchange of heliumlike ions is reproduced by the approximations (dotted, dashed, and dash-dotted lines, as labeled in Fig. 1). While the qualitative general trend is mostly reproduced, we note that, quantitatively, the fewer exact conditions an approximation satisfies, the higher the inaccuracy, which in fact increases as we move from MGGA to GGA to LDA. In particular, LDA becomes unable to reproduce, even qualitatively, the saturation to maximum distance, despite considering ion’s nuclear charges as large as $Z = 2000$.

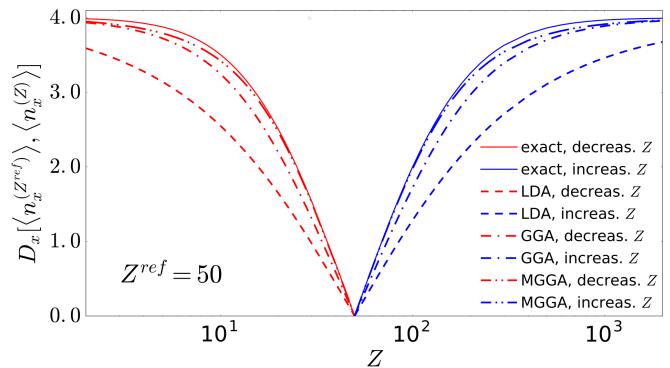


Figure 1. The x-hole distance D_x from the reference state $Z^{ref} = 50$ is plotted against the atomic number Z for the heliumlike ion series. The exact results correspond to the solid lines, LDA to the dashed lines, GGA to the dash-dotted lines, and MGGA to the dash-double-dotted lines.

Distances can also be used to perform “point-by-point” exact-to-approximated comparisons, by directly computing the distance between exact and approximated exchange for each system. Figure 2 shows the distances of approximated $\langle n_x \rangle$ from the corresponding exact quantity for each ion in the isoelectronic heliumlike sequence. As the electrons get strongly confined around the nucleus, the effect of the electron-electron interaction becomes negligible with respect to an external potential which increases linearly with Z . In this way, the noninteracting limit of an infinitely charged ion is approached. Interestingly, errors with respect to the exact results quickly saturate at a finite constant. For LDA and GGA, these errors may be mainly related to spurious self-interactions. Notably, although the considered MGGA gives rather accurate x energies for two-electron systems, it is obvious that a sizable error still persists at the level of $\langle n_x \rangle$. Importantly, the use of natural metrics allows us to *quantify* what we mean by “sizable,” by expressing the error as a *percentage of the maximum distance*. In the case at hand then, a 10% error threshold would correspond to $D_x = 0.4$ (dashed black line). We can then assert that for the heliumlike ion series, both GGA and MGGA always provide results which are closer than 10% to the exact ones (about 7.8% for GGA and between 4.0% and 3.0% for MGGA), while LDA estimates, at about 24.0% of D_x^{max} , are always well above the chosen error threshold.

Consistent with the general expectation, both in Fig. 2 and Fig. 1, the GGA performs in between the MGGA and LDA; however, our method and results show in an immediate and appealing visual way how substantial is the improvement obtained in going from an LDA to a GGA. The improvement of the MGGA over the GGA is not as large as from LDA to GGA, but still significant.

For DFT practitioners, it is important to clarify under which circumstances numerically “cheaper” approxima-

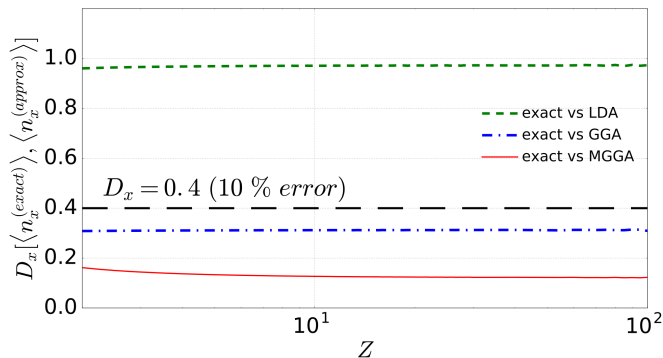


Figure 2. The x-hole distance D_x is plotted against the atomic number Z for the heliumlike ion series. For each Z , the distance is calculated between the exact x hole and several approximated x holes (LDA, GGA and MGGA), as labeled. The black dashed line represents 10% percent of the maximum distance from the exact x hole.

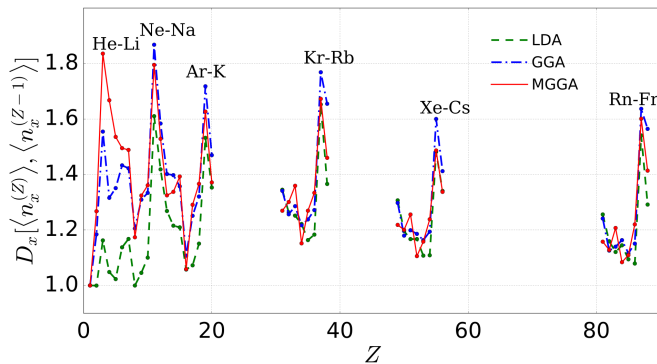


Figure 3. The x-hole distance D_x between atoms with atomic numbers Z and $Z-1$ is plotted against Z for the s and p blocks of the periodic table. The distances are calculated for LDA, GGA, and MGGA, as labeled. The distances between the end and the beginning of consecutive periods are explicitly labeled with the corresponding atoms. All the input Kohn-Sham quantities have been obtained using the APE code [19]. We allow for spin polarization by performing spin-DFT calculations [12]. We used logarithmic spaced grids and cubic spline interpolation [20] to calculate the x-hole distance between different atoms. All the densities and x-hole sum rules were tested within 10^{-4} .

tions could be used in place of more accurate but computationally more involved approaches. Toward this goal, in the rest of this paper, we show how the metric for the x hole can be used to efficiently compare the performance of different DFT approximations on large sets of systems. In the process, we will also show how D_x can be used to capture and compare physical trends within a large set of systems.

First we focus on physical trends within a set of systems, and so we consider distances between x holes of *different* systems calculated using the *same* approximation. Figure 3 shows distances between neutral atoms with atomic numbers Z and $Z-1$. Moving along the

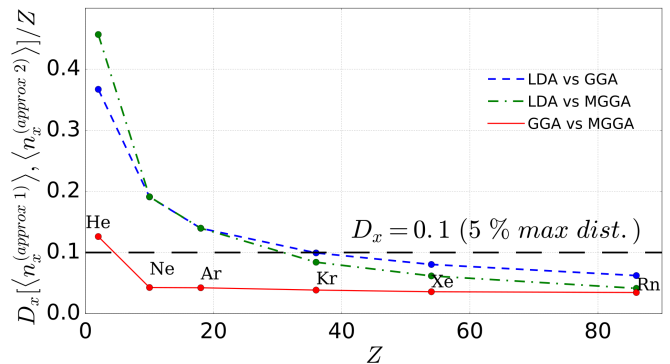


Figure 4. The x-holes distance D_x is plotted against the atomic number Z for the noble gas series. The distances are calculated between different approximations to the same x hole for all atoms, as labeled, and are rescaled by the number of electrons. The black dashed line marks 5% of the maximum possible distance. All the input Kohn-Sham quantities have been obtained using the APE code [19].

rows of the periodic table, the periodicity is well reflected in the behaviors of D_x for MGGA (solid line), the most accurate approximation considered here. For example, the curves characteristically peak when considering the distance between the x holes of the last atom of one row and the first of the next (as labeled in Fig. 3). This behavior follows from the sharp change of the corresponding atomic sizes. The MGGA curves also display characteristic minima at every start of double occupancy in spin of the p shells: as the fourth p electron is introduced, the atomic radius does not change significantly. This implies that the x-hole distance from the previous atom sharply decreases. Significant deviations are observed for LDA results for atoms in the first two rows. We explain this by noting that self-interaction errors become larger in small systems, and electrons of light elements tend to behave rather differently from the electrons in a homogenous gas. GGA improves over this by accounting better for density inhomogeneity, but it is still quite poor for the smaller Z values. For larger values of Z , the trends of LDA and GGA looks qualitatively more similar to MGGA results, although, as Z increases, maximum and minimum features related to the filling of the p shells get displaced with respect to MGGA positions.

Next, we wish to show how distances can lead to direct comparison between different approximations: here distances are calculated between *different* approximations applied to the *same* system, e.g., the same atom. In Fig. 4, we report these distances for the noble gases. The first thing to notice is that the distances among the various approximations decrease substantially with increasing Z . This is related to the fact that in all the considered approximations, the leading contribution to the semiclassical expansion of the exchange energies is provided through LDA [21]. The remaining differences can be attributed to high-orders contributions, more re-

lated to system inhomogeneities. Consistently, thus, the GGA and MGGA results are closer to each other than to the LDA. We can now define an error threshold to establish the parameter region for which LDA and GGA would be a good-enough cheaper substitute for MGGA. As our best results are already approximated, we consider in this case a threshold of 5% of the maximum possible distance, which corresponds in this case to $D_x/Z < 0.1$ (black dashed line in Fig. 4). It is immediate to see then that while LDA would be appropriate only for the heaviest three, GGA would be a good choice for all noble gases except helium.

IV. SUMMARY AND CONCLUSIONS

In summary, we have presented a way to rigorously and quantitatively compare exchange-only correlations of different systems. We have given evidence that by the use of a “natural” metrics, it is possible to effectively and efficiently characterize exchange-only correlations in many-electron systems. Our metric based on the exchange hole could have important practical applications in evaluating DFT approximations. For example, our results suggest that among the available approximations for the system-averaged exchange-hole, the meta-GGA performs best and could be used in evaluating distances for systems widely different in size and level of inhomogeneity. Our x-hole metric could also help guiding high-throughput materials design [22], e.g., for searching in large configurational spaces or for validating the reproducibility of a collaborative database of electronic calculations, independently from the different methodology, quantum package, or hardware used [23]. Natural metrics such as this or the one for the particle density [4] might also be used to ensure that newly developed functionals optimize, together with the total energies, other key physical quantities, helping revert the trend recently described in [24].

ACKNOWLEDGMENTS

We thank Professor Luiz Nunes de Oliveira for fruitful discussions. I.D. acknowledges support by the Royal Society through the Newton Advanced Fellowship scheme (Grant No. NA140436). I.D. and S.M. were supported by the Conselho Nacional de Desenvolvimento Científico e Tecnológico (Grant No. 401414/2014-0) and S.P. was supported by the European Community through the FP7s Marie-Curie International Incoming Fellowship, Grant agreement No. 623413.

-
- * simonemarocchi@ifsc.usp.br
 † stefano.pittalis@nano.cnr.it
 ‡ irene.damico@york.ac.uk
- [1] W. Kohn, Rev. Mod. Phys. **71**, 1253 (1999).
 - [2] K. Capelle, Braz. J. Phys. **36**, 1318 (2006).
 - [3] W. Koch and M. C. Holthausen, *A Chemists Guide to Density Functional Theory* (Wiley-VCH Verlag, Weinheim, 2001).
 - [4] I. D’Amico, J. P. Coe, V. V. França, and K. Capelle, Phys. Rev. Lett. **106**, 050401 (2011).
 - [5] P. M. Sharp and I. D’Amico, Phys. Rev. B **89**, 115137 (2014).
 - [6] P. M. Sharp and I. D’Amico, Phys. Rev. A **92**, 032509 (2015).
 - [7] P. M. Sharp and I. D’Amico, Phys. Rev. A **94**, 062509 (2016).
 - [8] D. P. Pires, M. Cianciaruso, L. C. Céleri, G. Adesso, and D. O. Soares-Pinto, Phys. Rev. X **6**, 021031 (2016).
 - [9] C. J. Turner, K. Meichanetzidis, Z. Papic, and J. K. Pachos, Nat. Commun. **8**, 14926 (2017).
 - [10] K. Funo, J.-N. Zhang, C. Chatou, K. Kim, M. Ueda, and A. del Campo, Phys. Rev. Lett. **118**, 100602 (2017).
 - [11] For the sake of simplicity, we restrict ourselves to the cases for which the Kohn-Sham state is a single Slater determinant.
 - [12] In the standard formulation of Kohn-Sham DFT, the occupation numbers $f_{k\sigma}$ take integer values (0 or 1). Fractional values are also admitted in the sense of its ensemble generalization. In this work, we restrict to closed-shell systems or to situations with globally collinear spin polarizations. In the latter case, one must take into consideration that the x hole acquires a dependence on the spin polarization. The spin-dependent x hole can be expressed in terms of the spin-unpolarized x hole by means of the spin-scaling relation [17, 25] as follows

$$n_x[n_\uparrow, n_\downarrow](\mathbf{r}, \mathbf{r}') = \sum_{\sigma} \frac{n_{\sigma}(\mathbf{r})}{n(\mathbf{r})} n_x[2n_{\sigma}](\mathbf{r}, \mathbf{r}').$$
 - [13] W. A. Sutherland, *Introduction to Metric and Topological Spaces* (Oxford University Press, Harvard, 2009).
 - [14] For discussing invariance under more general gauge transformations, one should admit additional couplings to proper external gauge fields and adopt the corresponding extensions of the DFT frameworks as done, for example, in current-DFT and spin-current-DFT(CDFT) [26–28].
 - [15] The onion-shell geometry characterizes *all* “natural” metrics, as a consequence of the protocol defined to derive them. A detailed discussion, including a discussion of the polar angle characterizing the distance between two systems, can be found in Ref. 5.
 - [16] M. Ernzerhof and J. P. Perdew, J. Chem. Phys. **109**, 3313 (1998).
 - [17] L. A. Constantin, J. P. Perdew, and J. Tao, Phys. Rev. B **73**, 205104 (2006).
 - [18] The isoelectronic heliumlike sequence was solved exactly combining the approaches taken by Accad et al. [29] and Coe et al. [30].
 - [19] M. J. T. Oliveira and F. Nogueira, Comp. Phys. Commun. **178**, 524 (2008).

- [20] P. Dierckx, *Curve and Surface Fitting with Splines* (Oxford University Press, New York, 1993).
- [21] P. Elliott and K. Burke, *Can. J. Chem.* **87**, 1485 (2009).
- [22] S. Curtarolo, G. L. W. Hart, M. B. Nardelli, N. Mingo, S. Sanvito, and O. Levy, *Nat. Mater.* **12**, 191 (2013).
- [23] C. E. Calderon, J. J. Plata, C. Toher, C. Oses, O. Levy, M. Fornari, A. Natan, M. J. Mehl, G. Hart, M. B. Nardelli, et al., *Comp. Mater. Science* **108, Part A**, 233 (2015).
- [24] M. G. Medvedev, I. S. Bushmarinov, J. Sun, J. P. Perdew, and K. A. Lyssenko, *Science* **355**, 49 (2017).
- [25] J. P. Perdew, K. Burke, and Y. Wang, *Phys. Rev. B* **54**, 16533 (1996).
- [26] G. Vignale and M. Rasolt, *Phys. Rev. Lett.* **59**, 2360 (1987).
- [27] G. Vignale and M. Rasolt, *Phys. Rev. B* **37**, 10685 (1988).
- [28] K. Bencheikh, *J. Phys. A: Math. Gen.* **36**, 11929 (2003).
- [29] Y. Accad, C. L. Pekeris, and B. Schiff, *Phys. Rev. A* **4**, 516 (1971).
- [30] J. P. Coe, K. Capelle, and I. D'Amico, *Phys. Rev. A* **79**, 032504 (2009).